Electronics and Electrical Engineering

AIMS Electronics and Electrical Engineering, 6(3): 285–295.
DOI: 10.3934/electreng.2022017
Received: 12 June 2022
Revised: 20 July 2022
Accepted: 08 August 2022
Published: 19 August 2022

http://www.aimspress.com/journal/ElectrEng

Research article

Highly sensitive optical MEMS based photonic biosensor for colon tissue detection

Raghunathareddy M V[1,*], Indumathi G[1] and Niranjan K R[2]

[1] Cambridge Institute of technology, Bangalore
[2] BMSCE, Bangalore

*** Correspondence:** Email: raghunathreddy.ece@cambridge.edu.in.

Abstract: Biological component of cells, protein has been effectively studied and investigated using biological sensors. Photonic crystal-based sensor is highly sensitive optical nanostructure it can be manipulated to affect the motion of photon for users' application. In the proposed work microcavity based photonic crystal biosensor has been designed and investigated for its different optical sensing evaluation parameters such as transmission efficiency, sensitivity, Q factor and peak resonant wavelengths. Sensor is designed and analyzed for early detection of colon cancer tissues in blood. Radius of defect micropillar has been increased from 0.16 μm to 0.19 μm. High Quality factor 10232 has been achieved with the micro pillar radius of 0.17 μm and sensitivity 700nm/RIU. Similarly, radius of 0.16 μm, 0.18 μm and 0.19 μm has attained quality factor and sensitivity such as 5324,7232,8343 and 111 nm/RIU, 320 nm/RIU and 340 nm/RIU respectively. Compared other work in literature, proposed work has shown better sensing capability. Designed sensor has shown remarkable output and feasibility for future fabrication.

Keywords: RIU-Refractive Index Unit; FDTD-Finite Difference Time domain; colon; photonic crystal; optical MEMS; tissue

1. Introduction

Photonic crystal incorporated biosensing structures hold promise to many aforementioned challenges. The photonic crystal is a periodic optical structure. These sensing structures will alter the

motion of photons in much similar to the way in which ionic lattices affect the motion of electronics in solid [1]. Two-dimensional photonic crystal structures are designed for sensing and differentiating cancerous and noncancerous cells. Change in the refractive index of the cancerous and noncancerous cells has shown a distinct shift in wavelength.

A wide range of bandgap is observed i.e., 1320nm to 1951nm [2]. The sensor bandgap obtained is in the range of 1100 nm to 1680 nm for the sensing structure designed by Kumar et.al. Sensor is designed for detecting cervical cancer cells in a blood sample. The sensitivity achieved by the sensor is 143 nm/RIU. 2D photonic crystal has shown high sensitivity of 4615.38 nm/RIU and a quality factor of 573. This sensor is designed for the detection of different types of brain cells [3]. A one-dimensional photonic crystal is used in the detection of tuberculosis. Defect layer thickness is increased in the optimization process of photonic crystal sensing system design. The structure has achieved a sensitivity of 1390 nm/RIU [4]. In another work, a peak resonant wavelength of 1.54964 μm was obtained and a transmission efficiency of 56% is achieved [5]. Using 2D Photonic crystal sensor different blood components were detected such as Biotin-Streptavidin, Bovine Serum Albumin, Cytop (polymer), Ethanol, Glucose solution (40 gm/100ml), Haemoglobin, Blood plasma, Polyacrylamide, Sylgard184, Urethane Di methacrylate, Water [6]. Meep tool is used to construct the 2D photonic crystal where it has been used. 2D photonic crystals are used in the detection of glucose in urine. Peak resonant frequency of 0.293716 - 0.294065 (in Meep units) is attained [7]. Optical sensing mechanisms with nanocavity resonator is used in the detection of protein concentration. Micro hole configuration is considered during the analysis of 2D photonic crystal simulation. The structure consists of two consecutive curves and a waveguide for the detection of glucose concentration in urine [8].

The photonic crystal ring resonator's structure has been designed and analyzed for a different configuration. Rings are formed in series and parallel. Photonic crystal in holes in slab and micro pillar configurations are investigated for the application of different pressure range [9]. A comprehensive review of different types of photonic sensor has been described in this research paper. Mainly photonic crystal, Mach Zehnder interferometers, Surface plasmon resonance and fibre Bragg grating sensors. Critical factors and future scope of these sensors are mentioned in detail [10]. Different types of microcantilever have been coupled with a photonic sensing layer. Rectangular, Triangular and trapezoidal microcantilever has been integrated with photonic sensing patches for detection of various of fluids such as air and water. High sensitivity is achieved with a regular triangular profile based photonic sensor [11]. Integrated photonic based microcantilever has been also investigated with applications such as colon cancer and prostate cancer. Here a number of Carcino embryonic antigen adhering to the surface of microcantilever is considered during the analysis [12,13].

As we can see from the literature photonic crystal biosensor is highly sensitive for change in refractive index. For a minute change in refractive index of biosample photonic crystal sensor exhibit large wavelength shift. The proposed work consists of design and development of a photonic crystal-based sensor for the early detection of colon cancer tissues. Using horizontal loop and vertical loop resonator in detecting of colon cancer new concept proposed in this work.

2. Design and working principle

In this proposed method, Finite Difference Time Domain (FDTD) is considered for solving the Maxwell equation. The sensing system is discretized. Discretized cell size is considered with the

different values with the FDTD solution.

The designed photonic crystal-based biosensor has silicon micropillar rods arranged in a hexagonal lattice configuration. In the hexagonal lattice configuration number of micropillar, in X and Z directions is given by 30 μm × 20 μm is shown in the Figure 1. The distance between each micropillar is 1 μm. Distance between micropillar is termed as lattice constant. A straight waveguide is formed by removing a specific micropillar in the straight-line path. The radius of the center micropillar is kept varied to identify the better sensing capability of sensors, such as sensitivity, operative wavelength range, Q factor, and transmission efficiency. The radius of the center micropillar varied from 0.16 μm to 0.19 μm. For the propagation inside the structure, 1550 nm wavelength is used. The monitor is used at the right end of the sensing system. Propagation of light inside the photonic crystal sensing system is given by the following method.

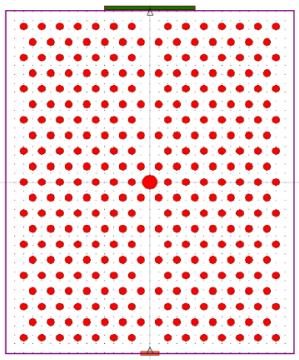

Figure 1. Sensing structure configuration designed in Rsoft tool.

$$\nabla \times \left(\frac{1}{\epsilon}\ [\ \nabla \times \mathrm{H}\ ]\right) = \left(\frac{\omega}{c}\right)^2 \mathrm{H} \tag{1}$$

In above maxwells electromagnetic equation stated Eq 1, ϵ is permittivity, ω is the angular frequency [6].

The quality factor is the second measuring factor in the design of a photonic crystal sensing system. The quality factor of the photonic crystal sensing system is found by the following equation i.e.,

$$\text{Quality factor} = \frac{\lambda}{FWHM} \tag{2}$$

The quality factor is the quantification of light transmitted from the input port to the output port. In the above equation, λ is peak resonant wavelength and FWHM is full width half maximum [6].

$$\mathrm{S} = \frac{\Delta\lambda}{\Delta n}\ \text{nm/RIU} \tag{3}$$

Δλ is the change in wavelength and Δn represents the change in refractive index of the biosample [6].

2.1. Type of cancer cells for analysis

A. Normal Colonic Mucosa

Normal colonic mucosa will be seen in pale pink color and can be commonly seen in the colon throughout the colon usually occurring in the rectum and cecum. Figure 2 shows the microscopical

image of normal colonic mucosa.

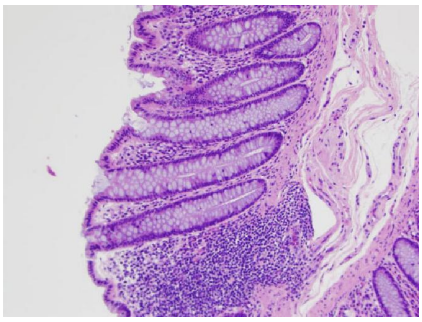

Figure 2. Normal colonic mucosa cell [14].

B. Tubulovillous Adenoma

A Tubulovillous adenoma is a non-cancerous growth in the colon. Usually develops in the glands of the colon and it also may appear anywhere between the rectum to cecum. Figure 3 shows the microscopic image of Tubulovillous adenoma.

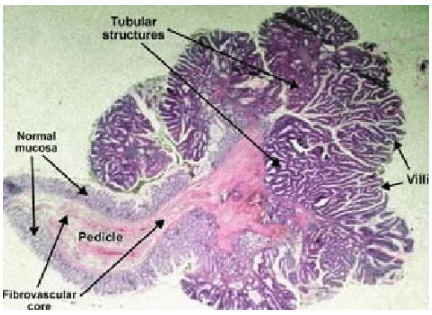

Figure 3. Tubulovillous adenoma cell [15].

C. Adenocarcinoma

It's a type of cancerous growth that develops in the lines and walls of the mucosal membrane of the colon in case of colon cancer.

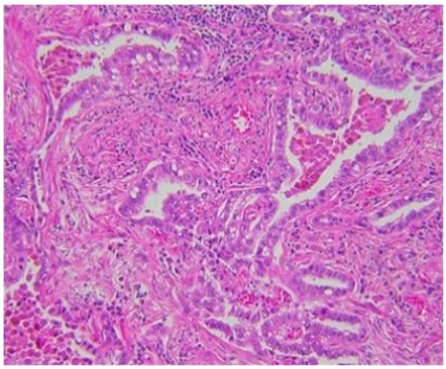

Figure 4. Microscopic image of adenocarcinoma cells [16,17].

Table 1. Refractive index of cancer cell [18,22–24].

Sl. No	Cancer cell	Refractive Index
1	Normal Mucosa (cecum)	1.329
2	Tubulovillous adenoma	1.348
3	Normal musoca (sigmoid)	1.337
4	Adenocarcinoma (tubulovillous background)	1.347

In Figure 5 blood samples of normal and abnormal conditions people with a refractive index of normal mucosa, Tubulovillous adenoma, normal mucosa in sigmoid regions, and adenocarcinoma with refractive indexes such as 1.329, 1.348, 1.337, 1.347 have channeled through microfluidic channels. Figure 6 investigated with the defect radius of 0.16 µm, 0.17 µm, 0.18 µm and 019 µm. Four resonance wavelengths are received at the output. This resonant wavelength represents the coon tissue conditions. Table 1 shows the refractive index of cancer cells.

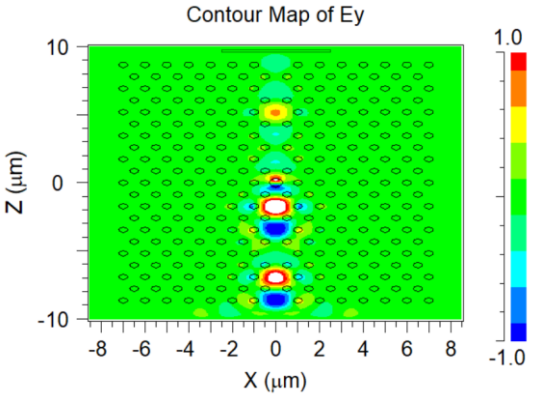

Figure 5. Light propagation in sensing structure.

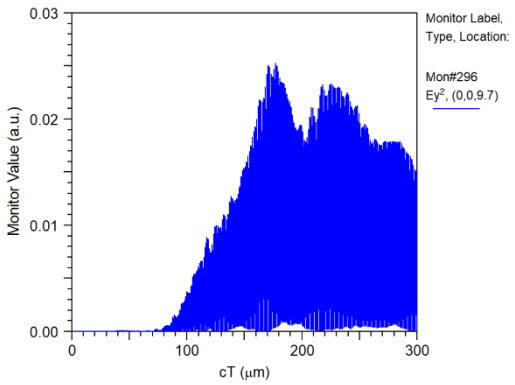

Figure 6. Monitor Output of light propagation.

3. Results and discussion

Sensor performances such as sensitivity, quality factor and peak resonant wavelength of proposed photonic biosensor is investigated with two-dimensional biosensing process. A gaussian light modulated wave are made pass through the waveguide designed and launched at the waveguide end at the input port with the wavelength of 1550 nm. The designed sensor has shown less loss as in all the micropillar radius various considered has shown transmission efficiency above 90%. Output signal is recorded by the output monitor. For normal mucosa peak resonant wavelength of 1234.8 nm is obtained and 1235.5 nm, 1236.4 nm, and 1236.8 nm for Tubulovillous adenoma, sigmoid normal mucosa and cancerous adenocarcinoma colon tissue respectively.

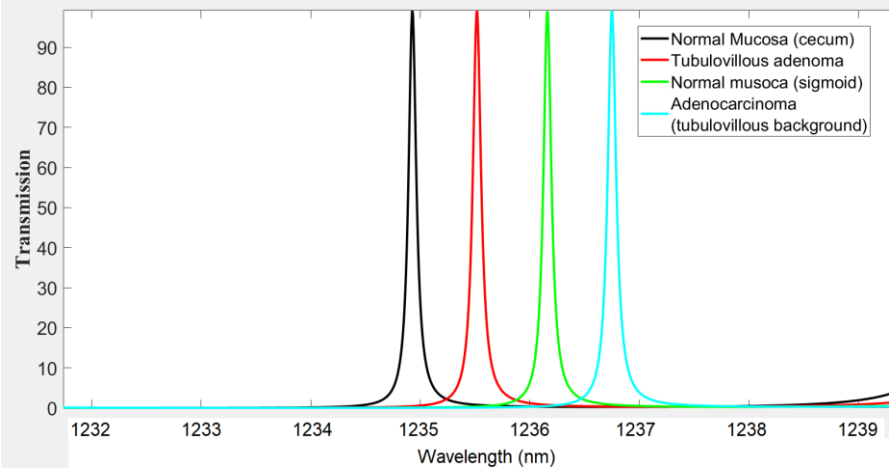

Figure 7. Transmission spectrum for defect radius micropillar 0.16 μm.

Table 2. Transmission spectrum data for defect radius micropillar 0.16 μm.

Sl. No	Colon tissues	Peak Resonant Wavelength	Q Factor	Sensitivity	Transmission efficiency
1	Normal Mucosa (cecum)	1234.8	5324		95
2	Tubulovillous adenoma	1235.5	5322		95
3	Normal musoca (sigmoid)	1236.4	5324	111 nm/RIU	95
4	Adenocarcinoma (tubulovillous background)	1236.8	5325		95

During the light propagation with radius of micropillar 0.16 μm optimum quality factor 5345 is generated. Maximum transmission efficiency such as above 95% and sensitivity of 560 nm/RIU. Normalized transmission spectrum obtained by above sensing configuration shown in Figure 7. High sensitivity of 111 nm/RIU is obtained for sensing pillar configuration with radius of 0.16 μm.

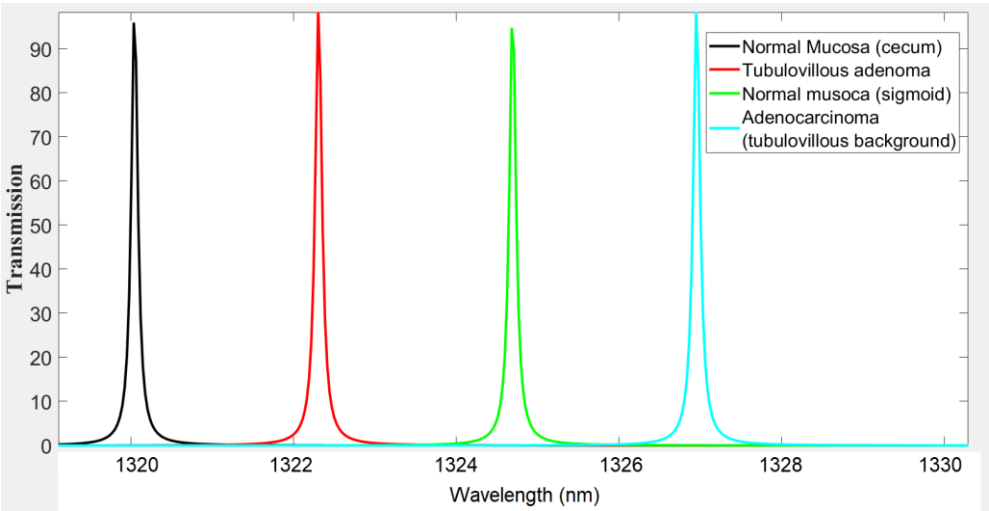

Figure 8. Transmission spectrum for defect radius micropillar 0.17 μm.

Table 3. Transmission spectrum data for defect radius micropillar 0.17 μm.

Sl. No	Colon tissues	Peak Resonant Wavelength	Q Factor	Sensitivity	Transmission efficiency
1	Normal Mucosa (cecum)	1320	10232		97
2	Tubulovillous adenoma	1322.4	10232	700 nm/RIU	97
3	Normal musoca (sigmoid)	1324.5	10232		97
4	Adenocarcinoma (tubulovillous background)	1327	10232		99

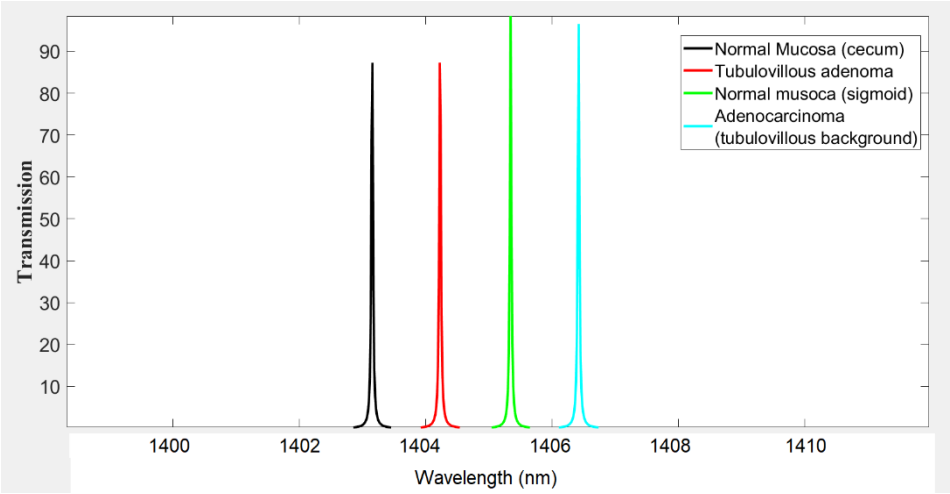

Figure 9. Transmission spectrum for defect radius micropillar 0.18 μm.

Figure 8, Figure 9 and Figure 10 show the transmission spectrum obtained for defect micropillar radius of 0.16 μm, 0.17 μm and 0.18 μm and 0.19 μm. It is observed from the results that maximum Q factor is obtained for microcavity radius of 0.17 μm and sensitivity of 700 nm/RIU. Quality factor 10232 was achieved for defect radius of 0.17 μm. 5325, 8343, 7232 achieved simultaneously changing the radius from 0.16 μm and 0.18 μm and 0.18 μm respectively. Transmission spectrum data for different radius of defect micropillar is shown in Table 2, Table 3, Table 4 and Table 5 respectively. As per the results obtained monitor power and peak resonant wavelength changes for changing the refractive index changes i.e., connected to defective microcavity. This helps identifying the different types of colon tissue and colon tissue with cancerous growth. The proposed sensor has shown linearity in peak resonant wavelength and its corresponding characteristics.

Photonic structural has high flexibility in forming the design due to the consideration of different parameters such as radius of micropillars, lattice constant, number of micropillars in configurations and different types of biosample with refractive index, length and width of waveguide etc.

Table 4. Transmission spectrum data for defect radius micropillar 0.18 μm.

Sl. No	Colon tissues	Peak Resonant Wavelength	Q Factor	Sensitivity	Transmission efficiency
1	Normal Mucosa (cecum)	1.403	8343		85
2	Tubulovillous adenoma	1.404.2	8343		85
3	Normal musoca (sigmoid)	1.405	8343	320 nm/RIU	98
4	Adenocarcinoma (tubulovillous background)	1.406.2	8343		96

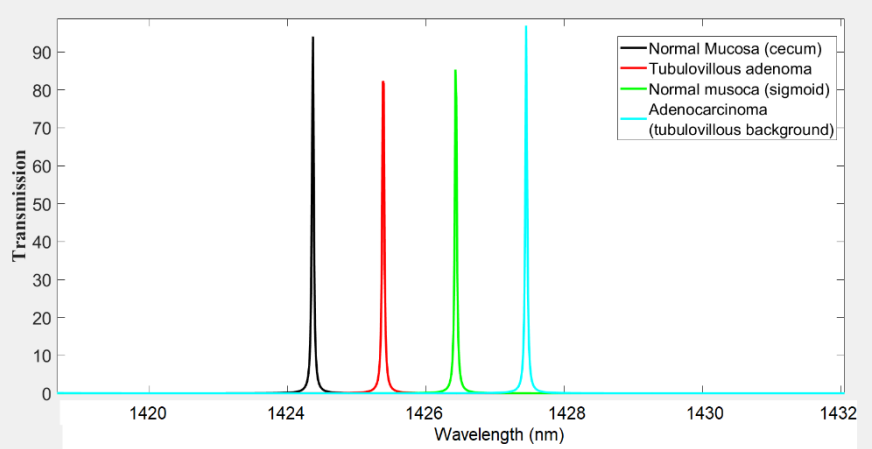

Figure 10. Transmission spectrum for defect radius micropillar 0.19 μm.

Table 5. Transmission spectrum data for defect radius micropillar 0.19 μm.

Sl. No	Colon tissues	Peak Resonant Wavelength	Q Factor	Sensitivity	Transmission efficiency
1	Normal Mucosa (cecum)	1424.3	7232		94
2	Tubulovillous adenoma	1425.3	7232		83
3	Normal musoca (sigmoid)	1426.4	7232	340	85
4	Adenocarcinoma (Tubulovillous background)	1427.6	7232		95

Table 6. Comparison of proposed work.

Ref. No	Year	Proposed Work	Remarks
[19]	2016	Photonic Crystal glucose monitoring	Sensitivity 422 nm/RIU
[20]	2021	Photonic crystal cancer cell detection	Sensitivity 300nm/RIU
[21]	2021	Creatinine detection	306.25nm/RIU
Present work	2022	Photonic crystal- colon tissue detection	700nm/RIU

4. Conclusions

In the proposed work microcavity based resonator has been designed and analyzed for the detection of abnormal colon tissue growths. Different types of micropillar radius have been considered for detection of abnormal tissue growth in colon. The radius of micropillar varied from 0.16 μm to 0.19 μm. It has been observed that quality factor of sensing configuration has been keep reduced as reduction defect micropillar radius from 0.17 μm to 0.19 μm. High quality factor 10232 achieved with the radius 0.17μm. The sensitivity of proposed sensor is 700 nm/RIU. For the proposed sensing configuration optimum radius of defect pillar will be 0.17 μm. Also, radius 0.17 μm has also shown feasible range of operative wavelength for respective refractive index range assisting the future fabrication possibility.

Acknowledgment

Author would like to thank all the researchers and staff of Cambridge Institute of technology for providing suggestions and ideas and support to carry out this research work and assisting in complete the manuscript successfully.

Conflict of interest

Authors declare there is no conflict of interest

References

1. Inan H, Poyraz M, Inci F, et al. (2017) Photonic crystals: emerging biosensors and their promise for point-of-care applications. *Chem Soc Rev* 46: 366–388. https://doi.org/10.1039/C6CS00206D
2. Sharma V, Kalyani VL, Upadhyay S (2017) Photonic crystal based bio-sensor detection in cancer cell using FDTD method. *2017 8th International Conference on Computing, Communication and Networking Technologies (ICCCNT)*, 1–5. https://doi.org/10.1109/ICCCNT.2017.8204043
3. Kumar H, Vaibav AM, Srikanth PC (2020) 2D Photonic Crystal based Biosensor for detection of Cervical Cancer cell. *2020 IEEE International Conference on Electronics, Computing and Communication Technologies (CONECCT)*, 1–4. https://doi.org/10.1109/CONECCT50063.2020.9198418
4. Aly AH, Mohamed D, Zaky ZA, et al. (2021) Novel Biosensor Detection of Tuberculosis Based on Photonic Band Gap Materials. *Materials Research*, 24. https://doi.org/10.1590/1980-5373-mr-2020-0483
5. Adoghe A, Noma-Osaghae E, Yabkwa R (2020) Photonic Crystal and its Application as a Biosensor for the Early Detection of Cancerous Cells. *International Journal of Online and Biomedical Engineering (iJOE)* 16: 86–94. https://doi.org/10.3991/ijoe.v16i03.12523
6. Sharma P, Roy SK, Sharan P (2014) Design and simulation of photonic crystal based biosensor for detection of different blood components. *2014 IEEE REGION 10 SYMPOSIUM*, 171–176. https://doi.org/10.1109/TENCONSpring.2014.6863019

7. Sharma P, Sharan P (2014) Photonic crystal-based sensor for detection of high glucose concentration in urine. *2014 Annual IEEE India Conference (INDICON)*, 1–6. https://doi.org/10.1109/INDICON.2014.7030390
8. Robinson S, Dhanlaksmi N (2017) Photonic crystal based biosensor for the detection of glucose concentration in urine. *Photonic Sens* 7: 11–19. https://doi.org/10.1007/s13320-016-0347-3
9. Patil PP, Kamath SP, Upadhyaya AM, et al. (2021) Design and analysis of photonic MEMS based micro ring resonators for pressure sensing application. *J Micromech Microeng* 31: 115004. https://doi.org/10.1088/1361-6439/ac2bb
10. Upadhyaya AM, Hasan MK, Abdel-Khalek S, et al. (2021) A Comprehensive Review on the Optical Micro-Electromechanical Sensors for the Biomedical Application. *Front Public Health* 9: 759032. https://doi.org/10.3389/fpubh.2021.759032
11. Upadhyaya AM, Srivastava MC, Sharan P (2021) Performance analysis of optomechanical-based microcantilever sensor with various geometrical shapes. *Microw Opt Technol Lett* 63: 1319–1327. https://doi.org/10.1002/mop.32652
12. Upadhyaya AM, Srivastava MC, Sharan P, et al. (2021) Silicon nanostructure-based photonic MEMS sensor for biosensing application. *J Nanophotonics* 15: 026001. https://doi.org/10.1117/1.JNP.15.026001
13. Upadhyaya AM, Srivastava MC, Sharan P (2021) Integrated MOEMS based cantilever sensor for early detection of cancer. *Optik* 227: 165321. https://doi.org/10.1016/j.ijleo.2020.165321
14. Smith CJ, Perfetti TA, King JA (2019) Rodent 2-year cancer bioassays and in vitro and in vivo genotoxicity tests insufficiently predict risk or model development of human carcinomas. *Toxicology Research and Application* 3: 2397847319849648. https://doi.org/10.1177/2397847319849648
15. Sopan S, Wickramaratne EKDM, Kotakadeniya HMSRB, et al. (2016) An unusually late presentation of malignancy in a patient with Gardner Syndrome. *Sri Lanka Journal of Medicine* 24: 28–32. http://doi.org/10.4038/sljm.v24i2.11
16. Lambe G, Durand M, Buckley A, et al. (2020) Adenocarcinoma of the lung: from BAC to the future. *Insights Imaging* 11: 1–10. https://doi.org/10.1186/s13244-020-00875-6
17. Parandin F, Heidari F, Rahimi Z, et al. (2021) Two-Dimensional photonic crystal Biosensors: A review. *Opt Laser Technol* 144: 107397. https://doi.org/10.1016/j.optlastec.2021.107397
18. Skivesen N, Tâu A, Kristensen M, et al. (2007) Photonic-crystal waveguide biosensor. *Opt Express* 15: 3169–3176. https://doi.org/10.1364/OE.15.003169
19. Mohamed MS, Hameed MFO, Areed NF, et al. (2016) Analysis of Highly Sensitive Photonic Crystal Biosensor for Glucose Monitoring. *The Applied Computational Electromagnetics Society Journal* (ACES), 31: 836–842.
20. Daher M, Taya SA, Colak I, et al. (2022) Highly Sensitive Nano-Biosensor Based on a Binary Photonic Crystal for Cancer Cell Detection. https://doi.org/10.21203/rs.3.rs-1218966/v1
21. Aly AH, Mohamed D, Mohaseb MA, et al. (2020) Biophotonic sensor for the detection of creatinine concentration in blood serum based on 1D photonic crystal. *RSC Adv* 10: 31765–31772. https://doi.org/10.1039/D0RA05448H
22. Konopsky VN, Karakouz T, Alieva EV, et al. (2013) Photonic Crystal Biosensor Based on Optical Surface Waves. *Sensors* 13: 2566–2578. https://doi.org/10.3390/s130202566

23. Ye C, Liang D, Ruan Y, et al. (2021) Photonic crystal barcode: An emerging tool for cancer diagnosis. *Smart Materials in Medicine* 2: 182–195. https://doi.org/10.1016/j.smaim.2021.06.003
24. Giannios P, Koutsoumpos S, Toutouzas KG, et al. (2017) Complex refractive index of normal and malignant human colorectal tissue in the visible and near-infrared. *J Biophotonics* 10: 303–310. https://doi.org/10.1002/jbio.201600001

AIMS Press